Preclinical Multimodal Molecular Imaging Using ^{18}F-FDG PET/CT and MRI in a Phase I Study of a Knee Osteoarthritis in In Vivo Canine Model

Maria I. Menendez, DVM, PhD[1], Bianca Hettlich, DrMedVet[1,2], Lai Wei, PhD[3], and Michael V. Knopp, MD, PhD[1]

Abstract

The aim of this study was to use a multimodal molecular imaging approach to serially assess regional metabolic changes in the knee in an in vivo anterior cruciate ligament transection (ACLT) canine model of osteoarthritis (OA). Five canine underwent ACLT in one knee and the contralateral knee served as uninjured control. Prior, 3, 6, and 12 weeks post-ACLT, the dogs underwent ^{18}F-fluoro-D-glucose (^{18}F-FDG) positron emission tomography (PET)/computed tomography (CT) and magnetic resonance imaging (MRI). The MRI was coregistered with the PET/CT, and 3-dimensional regions of interest (ROIs) were traced manually and maximum standardized uptake values (SUV_{max}) were evaluated. ^{18}F-fluoro-D-glucose SUV_{max} in the ACLT knee ROIs was significantly higher compared to the uninjured contralateral knees at 3, 6, and 12 weeks. Higher ^{18}F-FDG uptake observed in ACLT knees compared to the uninjured knees reflects greater metabolic changes in the injured knees over time. Knee ^{18}F-FDG uptake in an in vivo ACLT canine model using combined PET/CT and MRI demonstrated to be highly sensitive in the detection of metabolic alterations in osseous and nonosteochondral structures comprising the knee joint. ^{18}F-fluoro-D-glucose appeared to be a capable potential imaging biomarker for early human knee OA diagnosis, prognosis, and management.

Keywords

^{18}F-FDG, PET, MRI, osteoarthritis, knee, animal model

Introduction

Knee osteoarthritis (OA) is a common and debilitating disease that affects 27 million people in the United States.[1] Health-care expenditures of this condition have been estimated at US$186 billion annually.[2] The increasing importance of imaging OA for diagnosis, prognosis, and follow-up is well acknowledged. Although conventional radiography is the gold standard imaging technique for the evaluation of OA in clinical practice and in clinical trials, more sensitive imaging modalities are needed for the earlier diagnosis of OA. It is now widely agreed that OA is a disease of the whole joint. Magnetic resonance imaging (MRI) can assess all morphological structures of the joint, including cartilage, meniscus, ligaments, muscle, subarticular bone marrow, and synovium and thus can visualize the knee as a whole organ in 3 dimensions.[3] A comprehensive MR examination of the joint structures requires multiple sequences[2] and thus requires longer acquisition times. The MRI contrast agents such as ionic gadolinium chelates can be used to further evaluate cartilage composition (Delayed gadolinium enhanced Magnetic Resonance Imaging of cartilage [dGEMRIC]). Furthermore, it can detect microcirculation by dynamic contrast-enhanced MRI; however, these techniques increase the scan time and

[1] Department of Radiology, Wright Center of Innovation in Biomedical Imaging, The Ohio State University, Columbus, OH, USA
[2] Vetsuisse Faculty Bern, Bern, Switzerland.
[3] Center for Biostatistics, The Ohio State University, Columbus, OH, USA

Corresponding Author:
Maria I. Menendez, Department of Radiology, The Wright Center of Innovation in Biomedical Imaging, The Ohio State University, 395 W 12th Avenue, Columbus, OH 43210, USA.
Email: menendez.59@osu.edu

complexity[3] and fail to assess cell metabolism. Nuclear medicine and specifically positron emission tomography (PET)/computed tomography (CT) procedures using ^{18}F-fluoro-D-glucose (^{18}F-FDG) have been utilized to demonstrate metabolic changes in knee tissues, inflammation, and prosthesis infection.[4] Positron emission tomography/CT enables a pathophysiologic imaging and can provide different and complementary information than MRI. Increasingly, it can also be obtained at low radiotracer doses, thus reducing the ionizing radiation dose.[3] Although ^{18}F-FDG as a metabolic tracer is currently primarily used for oncologic diagnosis, therapy monitoring, and research, it has great potential for molecular musculoskeletal imaging.[4-7] The ^{18}F-fluoro-D-glucose PET can evaluate synovitis and bone marrow lesions associated with OA.[8] The ^{18}F-fluoro-D-glucose as a glucose analog cannot be further metabolized after phosphorylation and is trapped and accumulates within cells. This offers the opportunity to quantify ^{18}F-FDG PET uptake at sites of pathological increased glucose metabolism also in the musculoskeletal tissue. Glucose metabolism is affected by pro-inflammatory tumor necrosis factor α and increases in inflamed tissue,[9] making PET also a capable molecular imaging technique for the detection and quantification of inflammation.[10-12] Surgically induced OA has been used in animal models to study the pathogenesis of posttraumatic OA (PTOA). Dogs are the most widely used large animal model for translational research in OA compared to smaller species where macro- and microscopic anatomy, cartilage composition, and matrix turnover may significantly differ from that of humans.[13] The most commonly surgically created model used is the anterior cruciate ligament transection (ACLT). The results are highly reproducible and develop promptly.[13,14] The rationale for utilizing this model is that anterior cruciate ligament (ACL) injury causes joint destabilization, which subsequently leads to PTOA. In a mouse study using ^{18}F-FDG, Irmler et al showed a correlation of ^{18}F-FDG PET/CT uptake and histopathological evaluation of inflammatory experimental arthritis.[12] Paquet et al and Umemoto et al showed that ^{18}F-FDG uptake increased with the progression of arthritis in a rat arthritis model.[15,16] The ^{18}F-FDG PET has also proven its usefulness in diagnosing inflammation and infection in patients with painful hip and knee arthroplasties as well as rheumatoid arthritis.[17,18] Recently, ^{18}F-FDG PET uptake has been associated with age and OA.[19-21]

The advantages of ^{18}F-FDG PET/CT over conventional nuclear medicine techniques to assess inflammation and infection include higher sensitivity and better resolution images, improved target-to-background ratio, and faster scan times.[4,10] Moreover, heightened interest in the use of cross-sectional imaging techniques and their multimodal combination in clinical practice has led to combined hybrid modalities such as PET/CT and PET/MRI, largely because intraindividual comparative studies on the usefulness of combining functional and morphologic imaging for patients with OA have been lacking.

As far as we know, there is no published literature with regard to serial coregistered molecular imaging of both ^{18}F-FDG PET/CT and MRI in an in vivo canine model of OA. The aim of this study was to serially assess the metabolic activity in the knee, including both osseous and nonosteochondral structures, using a combination of 2 imaging modalities ^{18}F-FDG PET/CT and MRI in an in vivo ACLT canine model of OA. We hypothesized that the knees that underwent ACLT would show greater ^{18}F-FDG uptake than the uninjured knees.

Materials and Methods

Study Design

Procedures were approved by the local University Institutional Laboratory Animal Care and Use Committee. Five (n = 5) healthy, skeletally mature male beagles (age 5 years; weighing 10-13 kg) were used. All dogs were without any clinical and radiological signs of orthopedic disorders. The dogs were individually housed in indoor pens and were fed a standard diet with water ad libitum.

Induction of OA

Dogs underwent general anesthesia induced by acepromazine (intravenously (IV), 0.2 mg/kg; Vedco, Saint Joseph, Missouri), ketamine (IV, 6 mg/kg, Ketaset; Fort Dodge Animal Health, Overland Park, Kansas), and diazepam (IV, 0.35 mg/kg, Valium; Roche, Madison, Wisconsin) and maintained by isoflurane (Iso-Flo; Abbott, Parsippany, New Jersey; infusion, 2%-4%). Bilateral knee arthroscopy utilizing standard portals was performed to evaluate intra-articular structures. Using randomization, one knee had the ACL transected, while the ACL in the contralateral knee was left intact (uninjured). The contralateral knee arthroscopy was performed to evaluate knee structures and to balance possible effects of the arthroscopy procedure itself, such as swelling or effusion, on postoperative knee imaging.

Magnetic Resonance Imaging

Prior, 3, 6, and 12 weeks after ACLT, under general anesthesia, the canines underwent MRI. The MRI was performed using a 3-T MRI human whole-body system (Achieva; Philips Healthcare, Cleveland, Ohio) using an 8-channel knee coil. Dogs were placed in the supine position, with both knees extended in the knee coil. A custom-made table was used to ensure the same position in both the MRI and the PET/CT imaging. A clinical standard transaxial proton density (PD) turbo spin-echo (TSE) Spectral Presaturation with Inversion Recovery (SPIR) sequence was used (Echo time [TE] = 15 milliseconds, repetition time [TR] = 2100 milliseconds, flip angle 90°, slice thickness = 2 mm, field of view (FOV) = 115 mm, acquisition matrix: 144 × 124, voxel size: Foot-to-Head [FH] 0.56 mm, Anterior-to-Posterior [AP] 0.7 mm), followed by a sagittal PD TSE fat-saturated sequence (TE = 45 milliseconds, TR = 2200 milliseconds, flip angle: 90°, slice thickness: 2 mm, FOV = 88 mm; Figures 1 and 2).
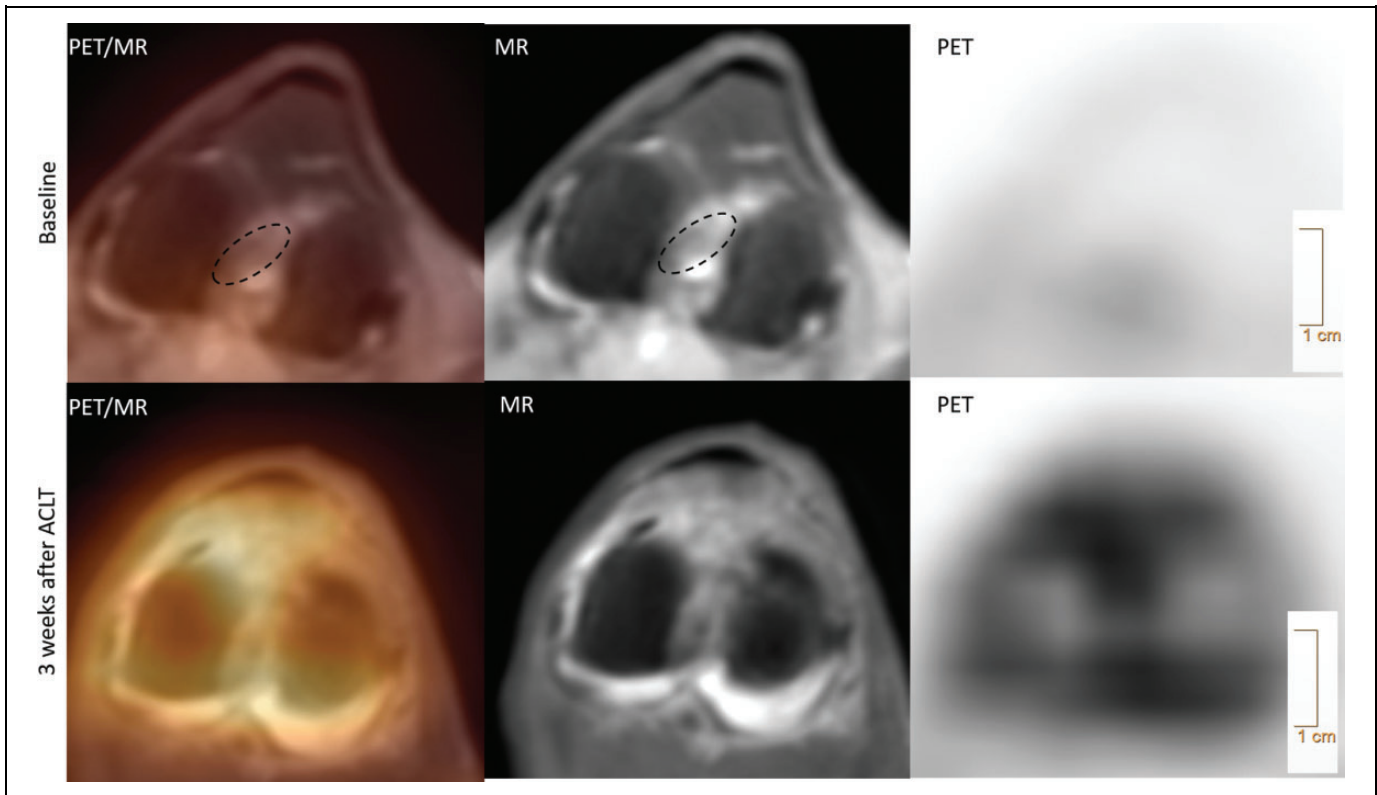
Figure 1. Representative knee PET/MR coregistered, MRI and ^{18}F-FDG PET (from left to right) transaxial views at baseline (top row), showing detailed knee morphology (ACL delineated in black dotted ellipse) and low ^{18}F-FDG uptake compared to 3 weeks post-ACLT (bottom row) showing higher ^{18}F-FDG uptake within the knee joint. At baseline, ^{18}F-FDG PET alone showed background uptake, making knee structure assessment challenging. ACLT indicates anterior cruciate ligament transection; ^{18}F-FDG, ^{18}F-fluoro-D-glucose; MRI, magnetic resonance imaging; PET, positron emission tomography.

Positron Emission Tomography/CT Imaging

Prior, 3, 6, and 12 weeks after ACLT, under general anesthesia, the dogs underwent ^{18}F-FDG PET/CT. Dogs fasted 6 hours prior to scan. They were kept in transport cages 4 hours prior to scan to limit physical activity. The participants were placed in the supine position in the custom-made table with both knees extended in the designed custom-made foam knee coil in order to mimic the same position as in the MRI knee coil and facilitate MRI coregistration. The table and foam knee coil together further helped to consistently coregister both modalities. Glucose levels were measured before 111 MBq (3 mCi) of ^{18}F-FDG was injected in the cephalic vein via IV catheter. The list mode time-of-flight raw data was acquired on the Gemini 64 TF with Astonish (Philips, Cleveland, Ohio) PET/CT system. Four millimeter isotropic voxel data sets (144×144 matrix size using a 576 mm FOV) and 90 seconds/bed were used. Images were reconstructed using the system default reconstruction parameters with the 4 mm voxel reconstruction (33 subsets and 3 iterations). Computed tomography was acquired using the multislice system at 120 KVp, 163 mAs and reconstructed with a 4-mm slice thickness (512×512 matrix size using 600 mm FOV) for attenuation correction and coregistration. Whole-body PET was acquired

30 minutes after ^{18}F-FDG administration for a duration of 20 minutes (Figures 1-3).

Positron Emission Tomography/MRI Analysis

The MRI and the PET/CT scans were performed in the same week for each time point. They were coregistered using the Philips IntelliSpace Portal workstation that uses an interpolation methodology to adjust for different matrix sizes. Three-dimensional (3-D) regions of interest (ROIs) were traced manually by one author (M.I.M.) to determine the SUV_{max} in a consistent way. Six-millimeter-diameter 3-D spheres were traced for the lateral femoral condyle, medial femoral condyle, lateral tibia, and medial tibia. Four-millimeter 3-D spheres were traced for the lateral meniscus and medial meniscus and 3-mm 3-D spheres were traced for the ACL and posterior cruciate ligament (PCL; Figure 2).

Statistical Analyses

The linear mixed-effect model was used to study the association between the type of treatment (ACLT and uninjured) and the SUV_{max} at each ROI and time point of the PET images, as well as the association of the SUV_{max} among the time points at
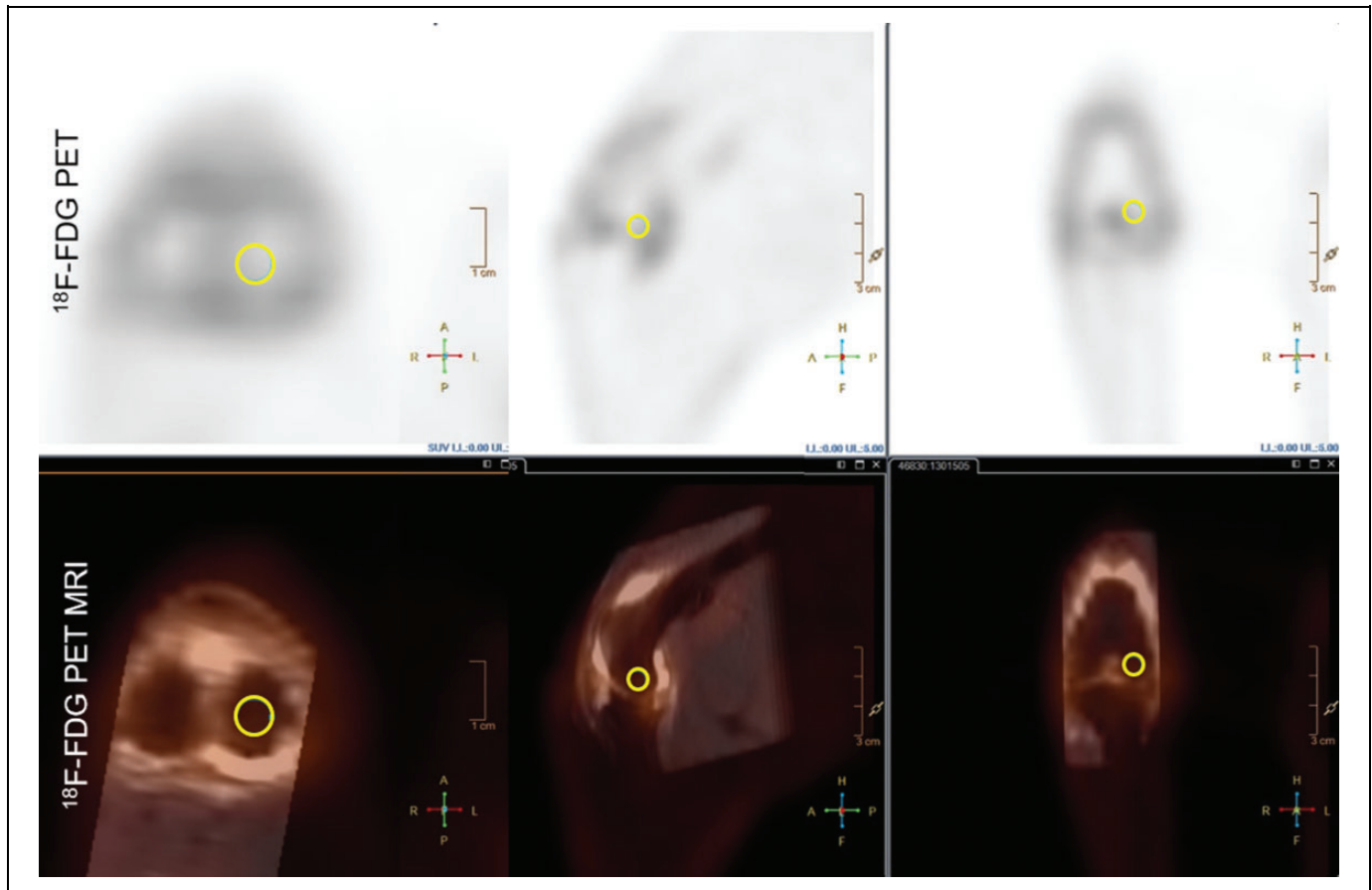
Figure 2. Representative ^{18}F-FDG PET (top) and ^{18}F-FDG PET/MRI coregistration (bottom) axial, sagittal, and dorsal views (from left to right) 3 weeks after ACLT. Showing the medial femoral condyle 3-D ROI (yellow circle) in the PET/MRI coregistered views, allowing for precise anatomic localization compared to the ^{18}F-FDG PET alone. ACLT indicates anterior cruciate ligament transection; ^{18}F-FDG, ^{18}F-fluoro-D-glucose; MRI, magnetic resonance imaging; PET, positron emission tomography.

each ROI for ACLT and uninjured, respectively. In addition, to determine correlation within and between dogs, the Holm-Bonferroni method was used to adjust for multiplicity. *P* values < .05 were considered statistically significant. Statistical analysis was performed using SAS v. 9.3 (SAS Institute, Cary, North Carolina).

Results

Magnetic resonance imaging and ^{18}F-FDG PET/CT scans were successfully completed prior, 3, 6, and 12 weeks after ACLT for all dogs, and all the image sets were successfully coregistered (Figures 1 and 2).

All the ROIs assessed in the ACLT knees compared to the uninjured knees presented with significantly higher FDG uptake quantified by SUV$_{max}$ at 3, 6, and 12 weeks (Figures 1-3; Table 1) including the lateral and medial femoral condyles, tibia, menisci, and PCL.

Comparing the FDG uptake in the different regions of the ACLT knees at 3, 6, and 12 weeks to baseline revealed significantly higher SUV$_{max}$ values also in the lateral and medial femoral condyles, lateral tibia, medial meniscus, and PCL (Figures 1-4; Table 2). For the medial tibia and lateral

meniscus, an elevated SUV$_{max}$ compared to baseline was found only at the later postinjury time points at 6 and 12 (Figure 4; Table 2).

Interestingly, the FDG uptake was elevated above baseline in all assessed regions (ROIs of bone, menisci, and PCL) in the ACLT knees at 12 weeks. On the other side, in the uninjured knees, FDG uptake returned to baseline levels at 12 weeks (Figure 4).

In the uninjured knees, the metabolic uptake in the lateral femoral condyle at 3 weeks was significantly higher relative to the later follow-up time points at 6 and 12 weeks. Also, the lateral meniscus presented significantly higher FDG uptake at 3 weeks compared to 6 and 12 weeks. The ACL at 3 weeks presented more intense FDG update (quantified by SUV$_{max}$) than at 12 weeks. The other regions presented elevated SUV$_{max}$ at 3 weeks relative to baseline, 6, and 12 weeks but were not statistically significantly different after adjusting for multiple comparisons (Figure 4; Table 2).

Discussion

Our findings demonstrate the feasibility of multimodal molecular imaging using ^{18}F-FDG PET/CT coregistered with MRI

Figure 3. Representative whole-body ^{18}F-FDG PET at baseline (A) and 3 weeks (dorsal and sagittal views, respectively (B and C) after ACLT. Red circles show increased ^{18}F-FDG uptake in the ACLT knee in comparison with the contralateral uninjured knee. ACLT indicates anterior cruciate ligament transection; ^{18}F-FDG, ^{18}F-fluoro-D-glucose; PET, positron emission tomography.

in the knee to serially assess and quantify metabolic changes in bone and nonosteochondral structures of the knee in a surgically induced (ACLT) canine model of OA.

At 3, 6, and 12 weeks, each assessed region in the ACLT knees had greater ^{18}F-FDG uptake than the uninjured knees. This finding is reflecting greater metabolic changes in the injured knees overtime relative to the uninjured knees due to the instability created by the ACL transection. The results are consistent with a similar study in patients with knee OA where the investigators also found higher metabolic uptake in whole joint ROIs in OA knees compared to uninjured knees.[21] The same study found ^{18}F-FDG uptake in the PCL and subchondral lesions in the OA knees that correlated with bone edema on the MRI. These results are consistent with a reported rat study where ^{18}F-FDG accumulation in arthritis reflected proliferating pannus and inflammatory activity enhanced by inflammatory cytokines, suggesting that ^{18}F-FDG μPET was effective for quantifying the

inflammatory activity of arthritis and/or its therapeutic response.[15] Moreover, ^{18}F-FDG PET uptake has been correlated with OA coupled with age and gender.[19,20]

[18]F-fluoro-D-glucose in ACLT knees did not return to baseline at 12 weeks due to the joint damage produced by ACL transection and the consequent OA initiation. Interestingly, the uninjured contralateral knees also presented elevated ^{18}F-FDG uptake at 3 weeks, returning to baseline levels at 6 and 12 weeks. This may be related to gait alterations due to joint instability induced by transecting the ACL, therefore shifting the dog's weight to the uninjured knee.

We chose arthroscopic surgery to deliver joint insults so as to minimize profound effects of arthrotomy on the joint, which may lead to substantial synovitis, hemorrhage, joint capsular fibrosis, and the associated pain and dysfunction. The dog is one of the most common studied species with respect to models of OA along with rabbits and rodents. Most importantly, clinical knee OA does occur in dogs due to

Table 1. ^{18}F-FDG Maximum Standardized Uptake Values (SUV$_{max}$) of 3-D Regions of Interest (ROIs) in the ACLT and the Uninjured Knee at Baseline, 3, 6, and 12 Weeks Post-ACLT.[a]

Assessed ROI	Timeline	ACLT SUV$_{max}$ Estimates (Mean $\pm$ SE)	Uninjured Estimates (Mean $\pm$ SE)	Linear Mixed Model *P* Value
Lateral femur	Baseline	0.47 $\pm$ 0.1	0.51 $\pm$ 0.07	.54
	3 weeks	2.52 $\pm$ 0.67	1.12 $\pm$ 0.25	.033[a]
	6 weeks	1.23 $\pm$ 0.08	0.46 $\pm$ 0.05	<.001[a]
	12 weeks	1.44 $\pm$ 0.15	0.48 $\pm$ 0.05	<.001[a]
Medial femur	Baseline	0.44 $\pm$ 0.07	0.39 $\pm$ 0.06	.06
	3 weeks	2.54 $\pm$ 0.63	0.99 $\pm$ 0.26	.009[a]
	6 weeks	1.29 $\pm$ 0.1	0.45 $\pm$ 0.05	<.001[a]
	12 weeks	1.3 $\pm$ 0.09	0.43 $\pm$ 0.05	<.001[a]
Lateral tibia	Baseline	0.41 $\pm$ 0.06	0.43 $\pm$ 0.03	.66
	3 weeks	2.42 $\pm$ 0.66	1.13 $\pm$ 0.33	.01[a]
	6 weeks	0.77 $\pm$ 0.07	0.36 $\pm$ 0.07	<.001[a]
	12 weeks	0.94 $\pm$ 0.12	0.47 $\pm$ 0.04	.007[a]
Medial tibia	Baseline	0.32 $\pm$ 0.04	0.35 $\pm$ 0.04	.26
	3 weeks	3.06 $\pm$ 1.03	1.07 $\pm$ 0.39	.033[a]
	6 weeks	0.1 $\pm$ 0.11	0.41 $\pm$ 0.05	.004[a]
	12 weeks	1.14 $\pm$ 0.11	0.36 $\pm$ 0.03	<.001[a]
Lateral meniscus	Baseline	0.43 $\pm$ 0.05	0.47 $\pm$ 0.04	.13
	3 weeks	2.28 $\pm$ 0.41	1.07 $\pm$ 0.23	.001[a]
	6 weeks	1.12 $\pm$ 0.07	0.42 $\pm$ 0.06	<.001[a]
	12 weeks	1.33 $\pm$ 0.12	0.47 $\pm$ 0.06	<.001[a]
Medial meniscus	Baseline	0.32 $\pm$ 0.03	0.4 $\pm$ 0.04	.008[a]
	3 weeks	2.66 $\pm$ 0.65	0.80 $\pm$ 0.17	.011[a]
	6 weeks	1.26 $\pm$ 0.07	0.42 $\pm$ 0.06	<.001[a]
	12 weeks	1.40 $\pm$ 0.12	0.4 $\pm$ 0.04	<.001[a]
PCL	Baseline	0.5 $\pm$ 0.06	0.51 $\pm$ 0.05	.65
	3 weeks	2.18 $\pm$ 0.40	1.06 $\pm$ 0.2	.003[a]
	6 weeks	1.51 $\pm$ 0.07	0.52 $\pm$ 0.06	<.001[a]
	12 weeks	1.54 $\pm$ 0.16	0.6 $\pm$ 0.07	<.001[a]

Abbreviations: ACLT, anterior cruciate ligament transection; 3-D, 3-dimensional; ^{18}F-FDG, ^{18}F-fluoro-D-glucose; PCL, posterior cruciate ligament; SE, standard error.
[a]*P* < .05 considered significant.

similar causes and results in similar signs and symptoms as is seen in humans.

Adding the MR coregistration enhances remarkably the ability to match anatomical structures to the metabolic PET maps. This is of paramount importance when assessing non-osteochondral structures, such as meniscus or ligaments. We utilized MRI in this study to advance the visualization and to accurately improve the localization of nonosteochondral knee tissues that otherwise could not have been delineated using PET/CT alone. The combination of these imaging modalities allowed precise assessment of different regions in the knee. In previous studies, ^{18}F-FDG uptake was assessed using the whole knee as 1 region[21] or only 2 regions segregating bone and soft tissue.[20] The authors were not able to evaluate different knee regions due to the inability to discriminate joint structures. The present study allowed us to delineate and assess precisely 3-D ROIs within the knee joint, including menisci and ligaments. As a result, we successfully were able to assess morphology in conjunction with quantitative metabolic activity.

The resolution provided by the PET/CT coregistration, which performs interpolation for matrix upscaling, was acceptable for this canine animal model. Due to the size of the dog knee, the 3-D ROIs applied (6, 4, and 3 mm) fall in the range of the PET voxel size used, which is a limitation. Our team is currently developing smaller voxel reconstruction methodologies (high-definition PET) that will facilitate more precise assessments in the future. Therefore, combined PET/CT and MR using ^{18}F-FDG as a tracer is a capable and detailed tool to quantify experimental joint metabolic changes accurately and noninvasively in vivo, as we demonstrated in this study.

Limitations of the study design have to be noted. We used the contralateral knee joint as the uninjured group instead of using control, nonoperated dogs. This minimized interanimal variation. The inclusion of control nonoperated dogs could provide additional insights into joint metabolic changes due to possibly altered limb loading patterns after ACLT in the contralateral joint. The study finalized 12 weeks after ACLT and thus does not give insight into even longer longitudinal changes. Further studies are needed with a larger dog population to elucidate the different joint metabolic changes that we observed in the ACLT and uninjured knees. Additionally, ^{18}F-FDG dose reduction and optimization should be considered
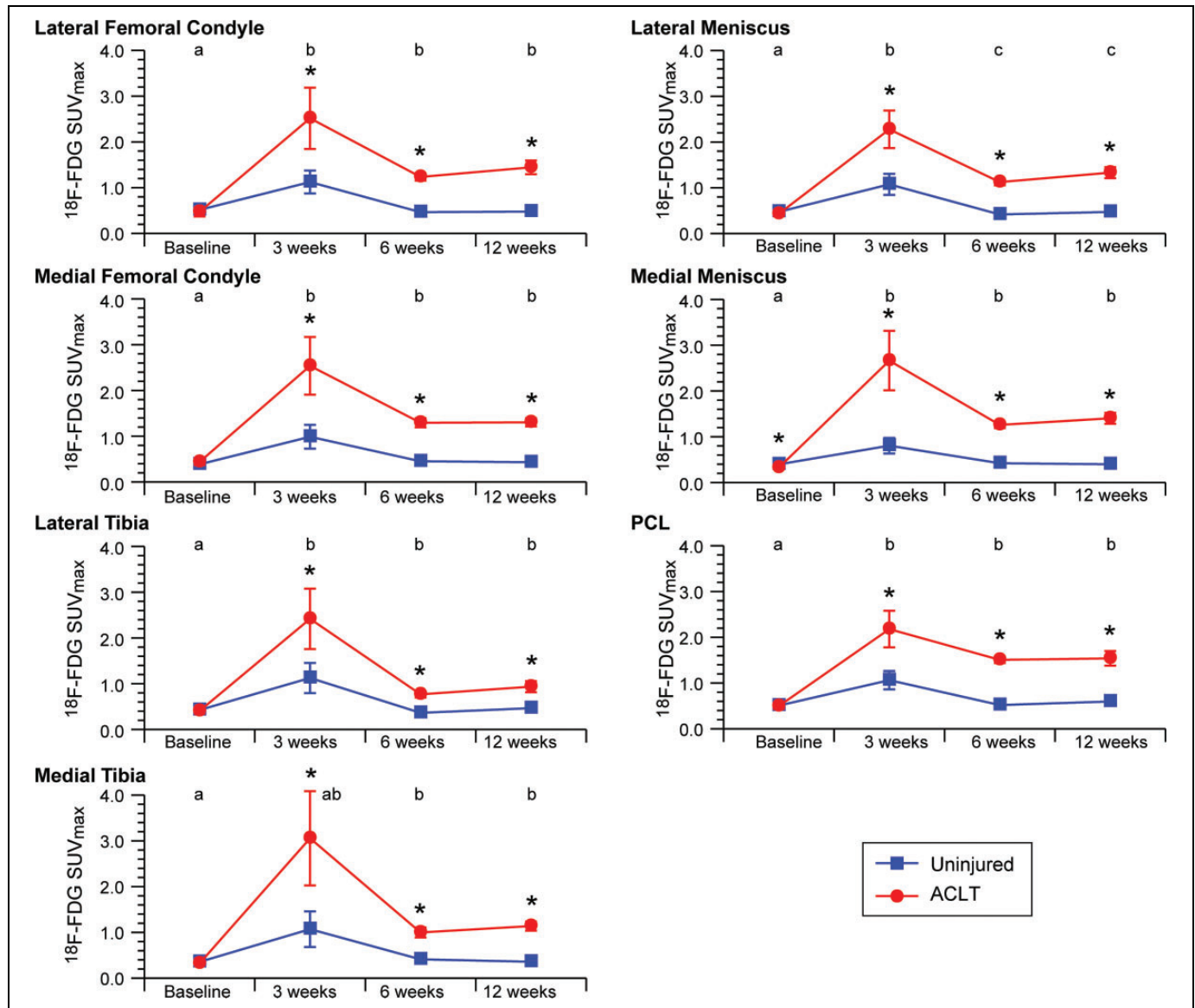
Figure 4. Region of interest (ROIs) ^{18}F-FDG SUVmax from the ACLT and uninjured knees at baseline, 3, 6, and 12 weeks. Data are expressed as mean $\pm$ SEM. Different letters comparing ACLT ROIs across time (A, B, and C) differ significantly ($P < .05$). Asterisks (*) shows significant difference between ACLT and uninjured knees. Posterior cruciate ligament (PCL). ACLT indicates anterior cruciate ligament transection; ^{18}F-FDG, ^{18}F-fluoro-D-glucose; SEM, standard error of the mean; SUV$_{max}$, maximum standardized uptake value.

in future studies to minimize staff radiotracer exposure and logistics burden.

[18]F-fluoro-D-glucose uptake of the knee in an in vivo ACLT canine model using PET-MRI coregistration demonstrated to be highly sensitive in the detection of metabolic alterations in different anatomical structures comprising the knee joint. Hence, ^{18}F-FDG uptake appears to be a potential imaging biomarker for an early OA diagnosis prior to the expression of morphologic changes, as well as a diagnostic tool to assess OA over time. In this study, we were able to prove our hypothesis that ACLT knees presented with greater ^{18}F-FDG uptake than the uninjured knees.

This study combined innovative multimodal molecular imaging techniques in a novel way to provide detailed,

comprehensive morphologic and metabolic information of the knee in an ACLT canine model of OA. It also confirmed that ^{18}F-FDG PET/CT coregistered with MRI can be used for serial quantitative assessment of early OA metabolic changes in osseous as well as nonosteochondral structures. The demonstrated methodology increases our knowledge of OA mechanisms at very early stages. The present findings highlight the importance of considering both molecular imaging and MRI to assess knee disorders that initiate OA. Further work is warranted to optimize the use of radiotracers in combination with MRI in translational research to diagnose PTOA. Overall, this study demonstrates the potential utility of FDG PET/CT combined with MRI for clinical OA research and patient management and is fully translatable to human applications.

Table 2. ^{18}F-FDG Maximum Standardized Uptake Values (SUV$_{max}$) of 3-D Regions of Interest (ROIs) in the ACLT Knee at Baseline, 3, 6, and 12 Weeks Post-ACLT and Multiple Comparisons *P* Values Using Holm-Bonferroni.[a]

Assessed ROI	Timeline	ACLT SUV$_{max}$ Estimates (Mean ± SE)	Holm-Bonferroni *P* Value
Lateral femur	3 weeks vs baseline	2.05 ± 0.70	.040[a]
	6 weeks vs baseline	0.76 ± 0.14	<.001[a]
	12 weeks vs baseline	0.97 ± 0.17	<.001[a]
	12 weeks vs 3 weeks	−1.07 ± 0.54	.2
	3 weeks vs 6 weeks	1.28 ± 0.69	.24
	12 weeks vs 6 weeks	0.21 ± 0.19	.87
Medial femur	3 weeks vs baseline	2.1 ± 0.66	.02[a]
	6 weeks vs baseline	0.86 ± 0.15	<.001[a]
	12 weeks vs baseline	0.87 ± 0.13	<.001[a]
	12 weeks vs 3 weeks	−1.23 ± 0.56	.13
	3 weeks vs 6 weeks	1.24 ± 0.55	.12
	12 weeks vs 6 weeks	0.01 ± 0.05	1
Lateral tibia	3 weeks vs baseline	2.01 ± 0.67	.03[a]
	6 weeks vs baseline	0.36 ± 0.08	.003[a]
	12 weeks vs baseline	0.53 ± 0.12	.003[a]
	12 weeks vs 3 weeks	−1.48 ± 0.6	.06
	3 weeks vs 6 weeks	1.65 ± 0.64	.06
	12 weeks vs 6 weeks	0.17 ± 0.15	.86
Medial tibia	3 weeks vs baseline	2.73 ± 1.06	.08
	6 weeks vs baseline	0.68 ± 0.12	<.001[a]
	12 weeks vs baseline	0.82 ± 0.13	<.001[a]
	12 weeks vs 3 weeks	−1.919 ± 1.02	.31
	3 weeks vs 6 weeks	2.06 ± 1.05	.27
	12 weeks vs 6 weeks	0.14 ± 0.07	.22
Lateral meniscus	3 weeks vs baseline	1.85 ± 0.38	<.001[a]
	6 weeks vs baseline	0.69 ± 0.09	<.001[a]
	12 weeks vs baseline	0.9 ± 0.1	<.001[a]
	12 weeks vs 3 weeks	−0.95 ± 0.35	.05[a]
	3 weeks vs 6 weeks	1.15 ± 0.43	.03[a]
	12 weeks vs 6 weeks	0.21 ± 0.18	.27
Medial meniscus	3 weeks vs baseline	2.34 ± 0.65	.01[a]
	6 weeks vs baseline	0.93 ± 0.07	<.001[a]
	12 weeks vs baseline	1.08 ± 0.11	<.001[a]
	12 weeks vs 3 weeks	−1.26 ± 0.56	.1
	3 weeks vs 6 weeks	1.40 ± 0.66	.2
	12 weeks vs 6 weeks	0.14 ± 0.13	.89
PCL	3 weeks vs baseline	1.68 ± 0.37	.001[a]
	6 weeks vs baseline	1.01 ± 0.05	<.001[a]
	12 weeks vs baseline	1.04 ± 0.14	<.001[a]
	12 weeks vs 3 weeks	−0.64 ± 0.25	.07
	3 weeks vs 6 weeks	0.67 ± 0.35	.22
	12 weeks vs 6 weeks	0.03 ± 0.11	1

Abbreviations: ACLT, anterior cruciate ligament transection; 3-D, 3-dimensional; ^{18}F-FDG, ^{18}F-fluoro-D-glucose; PCL, posterior cruciate ligament; SE, standard error.
[a]*P* < .05 considered significant.

References

1. Kotlarz H, Gunnarsson CL, Fang H, Rizzo JA. Insurer and out-of-pocket costs of osteoarthritis in the US: evidence from national survey data. *Arthritis Rheum*. 2009;60(12):3546–3553.
2. Hayashi D, Roemer FW, Guermazi A. Imaging for osteoarthritis. *Ann Phys Rehabil Med*. 2016;59(3):161–169.
3. Guermazi A, Roemer FW, Crema MD, Englund M, Hayashi D. Imaging of non-osteochondral tissues in osteoarthritis. *Osteoarthritis Cartilage*. 2014;22(10):1590–605.
4. Hess S, Hansson SH, Pedersen KT, Basu S, Høilund-Carlsen PF. FDG-PET/CT in infectious and inflammatory diseases. *PET Clin*. 2014;9(4):497–519, vi–vii.
5. Glaudemans AW, de Vries EF, Galli F, Dierckx RA, Slart RH, Signore A. The use of (18)F-FDG-PET/CT for diagnosis and treatment monitoring of inflammatory and infectious diseases. *Clin Dev Immunol*. 2013;2013:623036.
6. Imperiale A, Federici L, Lefebvre N, et al. F-18 FDG PET/CT as a valuable imaging tool for assessing treatment efficacy in inflammatory and infectious diseases. *Clin Nucl Med*. 2010;35(2):86–90.
7. Lawrence J, Rohren E, Provenzale J. PET/CT today and tomorrow in veterinary cancer diagnosis and monitoring: fundamentals, early results and future perspectives. *Vet Comp Oncol*. 2010;8(3):163–187.
8. Ju JH, Kang KY, Kim IJ, et al., Visualization and localization of rheumatoid knee synovitis with FDG-PET/CT images. *Clin Rheumatol*. 2008;27(suppl 2):S39–S41.
9. Yamada S, Kubota K, Kubota R, Ido T, Tamahashi N. High accumulation of fluorine-18-fluorodeoxyglucose in turpentine-induced inflammatory tissue. *J Nucl Med*. 1995;36(7):1301–1306.
10. Jones HA, Cadwallader KA, White JF, Uddin M, Peters AM, Chilvers ER. Dissociation between respiratory burst activity and deoxyglucose uptake in human neutrophil granulocytes: implications for interpretation of (18)F-FDG PET images. *J Nucl Med*. 2002;43(5):652–657.
11. Deichen JT, Prante O, Gack M, Schmiedehausen K, Kuwert T. Uptake of [^{18}F] fluorodeoxyglucose in human monocyte-macrophages in vitro. *Eur J Nucl Med Mol Imaging*. 2003;30(2):267–273.
12. Irmler IM, Opfermann T, Gebhardt P, et al. In vivo molecular imaging of experimental joint inflammation by combined (18)F-FDG positron emission tomography and computed tomography. *Arthritis Res Ther*. 2010;12(6):R203.
13. Kuyinu EL, Narayanan G, Nair LS, Laurencin CT. Animal models of osteoarthritis: classification, update, and measurement of outcomes. *J Orthop Surg Res*. 2016;11(1):19.

14. Cook JL, Kuroki K, Visco D, Pelletier JP, Schulz L, Lafeber FP. The OARSI histopathology initiative—recommendations for histological assessments of osteoarthritis in the dog. *Osteoarthritis Cartilage*. 2010;18(suppl 3):S66–S79.

15. Paquet J, Maskali F, Poussier S, et al. Evaluation of a rat knee mono-arthritis using microPET. *Biomed Mater Eng*. 2010;20(3): 195–202.

16. Umemoto Y, Oka T, Inoue T, Saito T. Imaging of a rat osteoarthritis model using (18)F-fluoride positron emission tomography. *Ann Nucl Med*. 2010;24(9):663–669.

17. Reinartz P. FDG-PET in patients with painful hip and knee arthroplasty: technical breakthrough or just more of the same. *Q J Nucl Med Mol Imaging*. 2009;53(1):41–50.

18. Zajonz D, Wuthe L, Tiepolt S, et al. Diagnostic work-up strategy for periprosthetic joint infections after total hip and knee arthroplasty: a 12-year experience on 320 consecutive cases. *Patient Saf Surg*. 2015;9:20.

19. Saboury B, Parsons MA, Moghbel M, et al. Quantification of aging effects upon global knee inflammation by ^{18}F-FDG-PET. *Nucl Med Commun*. 2016;37(3):254–258.

20. Hong Y, Kong E. (^{18}F)Fluoro-deoxy-D-glucose uptake of knee joints in the aspect of age-related osteoarthritis: a case-control study. *BMC Musculoskelet Disord*. 2013;14:141.

21. Nakamura H, Masuko K, Yudoh K, et al. Positron emission tomography with ^{18}F-FDG in osteoarthritic knee. *Osteoarthritis Cartilage*. 2007;15(6):673–681.